Original scientific paper
UDC: 66.018.9:666.32+66.081:67.017
DOI: 10.7251/afts.2017.0916.065D
COBISS.RS-ID 6440472

BENTONITE/IRON OXIDE MAGNETIC COMPOSITES: CHARACTERIZATION AND APPLICATION AS Pb(II) ADSORBENTS

Danková Zuzana[1], Fedorová Erika[1], Bekényiová, Alexandra[1]

[1]*Institute of Geotechnics, Slovak Academy of Sciences Košice, Slovak Republic, E-mail: orolinova@saske.sk*

ABSTRACT

The natural clay bentonite (B) as adsorbent of lead cations was studied. To enhance its adsorption capacity, the coating by iron oxide particles, in two selected weight ratios: 2:1 (BM1) and 4:1(BM2), was used. The changes of the textural and surface parameters after the modification were studied by the low temperature nitrogen adsorption, XRD and SEM method, Mössbauer spectroscopy. The Pb(II) adsorption experiments were studied under the different conditions, such as pH of the model solutions, contact time and initial metal ion concentration. Higher adsorption rates of BM1 and BM2 samples were observed for lower initial metal ion concentrations.

Keywords: *bentonite, composite, structural properties, adsorption.*

INTRODUCTION

Lead is a naturally occurring toxic metal found in the Earth's crust. Important sources of environmental contamination include mining, smelting, manufacturing and recycling activities, and, in some countries, the continued use of leaded paint, leaded gasoline, and leaded aviation fuel. More than three quarters of global lead consumption is for the manufacture of lead-acid batteries for motor vehicles. Lead is, however, also used in many other products, for example pigments, paints, solder, stained glass, crystal vessels, ammunition, ceramic glazes, jewelry, toys and in some cosmetics and traditional medicines. Drinking water delivered through lead pipes or pipes joined with lead solder may contain lead. Much of the lead in global commerce is now obtained from recycling. Once lead enters the body, it is distributed to organs such as the brain, kidneys, liver and bones. Lead exposure also causes anaemia, hypertension, renal impairment, immunotoxicity and toxicity to the reproductive organs [1].

The presence of negative charge on the surface of smectites is responsible for their good sorption properties. This makes natural bentonite a potential candidate for removal of heavy metals from wastes [2-7]. Besides the natural bentonite, other forms of bentonite modification which enhance some of its properties are used as: chemical treatment with acids, nitrification, pillaring of interlayer space with cations (Al), intercalation by organic cations and magnetic modification [8-21]. Surface decoration of the aluminosilicate minerals with magnetic nanoparticles had led to a new class of

composite materials, which could be also used for the environmental purposes as adsorbents of the organic and inorganic compounds and metal ions [22-25].

This paper deals with the structural and surface characterization of composite materials prepared by magnetic modification of the natural clay and their application as potential adsorbents of heavy metal cations.

EXPERIMENTAL

Bentonite, containing montmorillonite with crystalochemical formula: $[Si_{7.95}\,Al_{0.05}]\,[Al_{3.03}\,Fe_{0.22}\,Mg_{0.75}]\,O_{20}\,(OH)_4\,(Ca_{0.42}Mg_{0.04}Na_{0.01}K_{0.01})$, originated from the Slovak deposit Jelšový potok [26]. The composite materials were prepared by the method of precipitation of the iron oxide on the bentonite surface from the solution of $FeSO_4.7H_2O$ and $FeCl_3.6H_2O$ (with ratio of Fe^{3+}/Fe^{2+} = 2) in acidic condition by continuous stirring for 0.5 h in the nitrogen atmosphere at the ambient temperature [27]. The bentonite was mixed into the solution of ferrous and ferric salts prior to the reaction with NH_4OH and its amount was adjusted to obtain the bentonite/iron oxide weight ratios 2:1 and 4:1 (denoted BM1 and BM2 respectively). Then the dark brown suspension was stirred for half an hour. The final products were washed with deionised water, filtrated and dried at 70 °C.

The powder X-ray diffraction (XRD) patterns of natural bentonite and composite materials were recorded using a Philips PW1820 diffractometer (The Netherlands) equipped with a CuKα radiation (40 kV, 40 mA). The data were analysed using Philips Software, X'PertHigh Score with PDF-2 Database.

The Mössbauer measurements were made in transmission geometry. A ^{57}Co/Rh-ray source was used. The velocity scale was calibrated relative to ^{57}Fe in Rh. Mössbauer spectral analysis software "Recoil" [28] was used for the quantitative evaluation of the spectra. The Voigt-based fitting method was applied for all spectra to determine the line positions, line widths and peak intensities.

The value of magnetization of the samples was determined by the superconducting quantum interference device (SQUID) magnetometer measurement. The value of saturation magnetization was determined at the maximum field of 50 kOe.

The morphology of the natural bentonite and composite samples was observed by the field emission scanning electron microscope TESCAN MIRA3 (TESCAN, s.r.o. Brno, Czech Republic).

Surface properties of studied samples were determined from the adsorption and desorption isotherms measured with the NOVA 1200e Surface Area & Pore Size Analyzer (Quantachrome Instruments, USA) by the method of physical adsorption of nitrogen at -196 °C. First, the samples were degassed at 100 °C in a vacuum oven under a pressure lower than 2 Pa for 16 hours. The measured data were processed by the BET (Brunnauer–Emmet–Teller) isotherm in the range of relative pressure 0.05-0.3 to obtain the value of specific surface area (S_A). The values of external surface (S_{ext}) and volume of micropores (V_{micro}) were calculated from the t-plot using the Harkins-Jura standard isotherm. The value of total pore volume (V_{tot}) was estimated from the maximum adsorption at relative pressure close to saturation pressure. The pore size distribution was obtained from the desorption isotherm using the Barrett-Joyner-Halenda method [29].

The analytical grade metal salt ($Pb(NO_3)_2$ was used without the further purification. Stock solutions (1000 mg L^{-1} and 100 mg L^{-1}) of Pb(II) were prepared by dissolving the appropriate amounts of nitrate in de-ionized water. The stock solutions were diluted to obtain the standard solutions containing 10-500 mg Pb(II) L^{-1}. Through the study, the pH of the solutions varied from 2 to 9. The amount of adsorbent mass was stable 1 g L^{-1}. The suspensions were subsequently filtered using the filter paper, and the supernatant solutions were analyzed by the atomic absorption spectroscopy (AAS, Varian 240 RS/2400).

RESULTS AND DISCUSSIONS

Composites characterization

The XRD measurement of the natural bentonite confirmed the dominant montmorillonite phase in the sample, Fig. 1. The iron oxide particles were synthesized without the bearer and characterized by same methods to better interpret the changes of the surface and porous structure of bentonite after the modification. The XRD analysis of Fe oxide showed the reflections common for maghemite (γ-Fe_2O_3) and magnetite (Fe_3O_4). The XRD analysis of the composite materials confirmed the occurrence of Fe oxidized phase with reflection on planes (220), (311), (400), (422), (511) and (440). Except that the goethite phase (α-FeOOH) was observed for BM1 and BM2 materials.

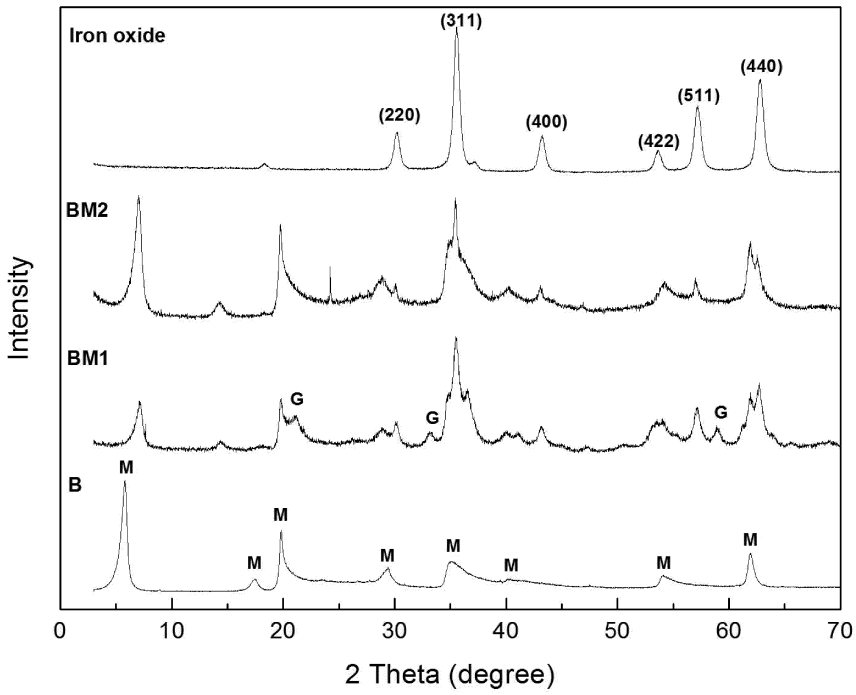

Figure 1 XRD pattern of natural bentonite, composite materials and iron oxide
(M – montmorillonite, G - goethite)

To determine the present iron oxide phase in the composite samples, Mössbauer spectroscopy was used. The bentonite/iron oxide composites spectra were complexes consisting of the central paramagnetic doublet and one sextet. The intensity of peaks of magnetically and non-magnetically oriented phases showed the dependence on the amount of present iron oxide phases. For the BM2 material, the sextet line was wider and the peaks intensity decreased in comparison to spectrum of BM1 material. Contrary, the intensity of central doublet increased. For the fitting, two sextets and two doublets - two paramagnetic positions of Fe^{3+} in bentonite were used [30-32]. The fitting of the spectra was completed by the third sextet subspectrum, corresponding to the present goethite phase, what was also confirmed by XRD. The demonstrations of fitted Mössbauer spectra are showed on Figs. 2-3 and fitted Mössbauer parameters for BM2 composite material are listed in Table 1.

The measured value of magnetization of iron oxide synthesized without the bearer was used to calculate the expected mass magnetization of composite samples, Table 2. The synthesized iron oxide particles showed magnetization of 83.59, which is similar to γ-Fe_2O_3 [33], and is smaller than theoretical (87.3 emu/g) confirming the nanoscale character of iron oxide particles. The content of magnetic phase in natural clay depends on the locality of deposit and contributes to whole value of magnetization. Usually it is about 3 – 3.5 % of Fe_2O_3 for this deposit [34]. The presence of trivalent

iron in bentonite was confirmed by the XRD and Mössbauer spectroscopy. The values of mass magnetization σ of composites correspond with their content of magnetic phase and are lower than theoretical. It should be caused by the presence of goethite in their structures.

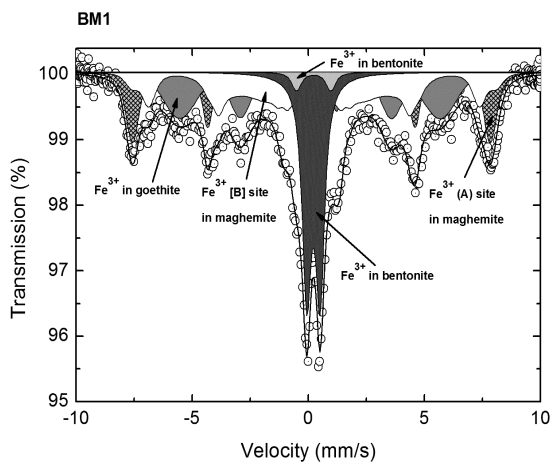

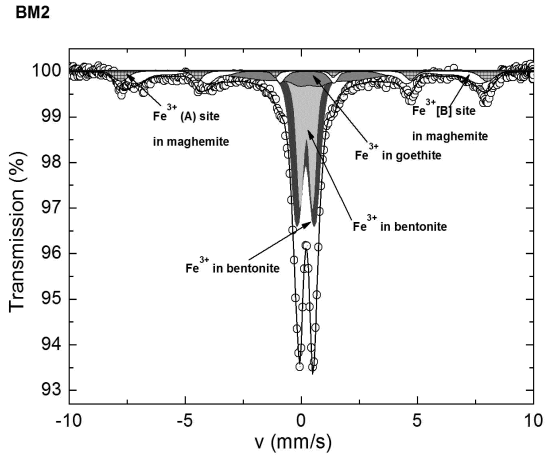

Figure 2 (left) Fitted Mössbauer spectrum of composite sample BM1
Figure 3 (right) Fitted Mössbauer spectrum of composite sample BM2

Table 1 Mössbauer parameters for composite material BM2

Sample		B_{hf} (T)	IS (mm/s)	QS (mm/s)	I (%)
BM2	Fe^{3+}		0.22	0.54	23.0
	Fe^{3+}		0.19	0.76	38.7
	Mh^{Tet}	49.0	0.13		6.9
	Mh^{Oct}	49.6	0.25		0.5
		46.0			12.1
		37.0			3.5
	G	15.3	0.26	-0.1	15.3

B_{hf} - hyperfine magnetic field, IS - isomer shift, I - relative spectral area, Fe^{3+} - position of trivalent iron in bentonite, Mh^{Tet}, Mh^{Oct} – tetrahedral and octahedral position of trivalent iron in maghemite, G – position of trivalent iron in goethite

The measured value of magnetization of iron oxide synthesized without the bearer was used to calculate the expected mass magnetization of composite samples, Table 2. The synthesized iron oxide particles showed magnetization of 83.59, which is similar to γ-Fe_2O_3 [33], and is smaller than theoretical (87.3 emu/g) confirming the nanoscale character of iron oxide particles.

The content of magnetic phase in natural clay depends on the locality of deposit and contributes to whole value of magnetization. Usually it is about 3 – 3.5 % of Fe_2O_3 for this deposit [34]. The presence of trivalent iron in bentonite was confirmed by the XRD and Mössbauer spectroscopy. The values of mass magnetization σ of composites correspond with their content of magnetic phase and are lower than theoretical. It should be caused by the presence of goethite in their structures.

Table 2 Theoretical and measured values of mass magnetization of natural bentonite, iron oxide and composite samples

Sample	Theoretical σ (emu/g)	Measured σ (emu/g)
Bentonite		4.02
Iron oxide	-	83.59
BM1	27.86	17.20
BM2	16.72	10.30

A detail of the morphology of BM1 material observed by SEM is shown in Fig. 4. The presence of iron in the modified sample was also confirmed by EDX analyses. The mapping mode was used for the separation of the composition contrast. The grey spots points represent the iron oxide particles covering the bentonite surface, Fig. 5. Generally the average size of magnetic particles in composites materials was in the range 10-30 nm.

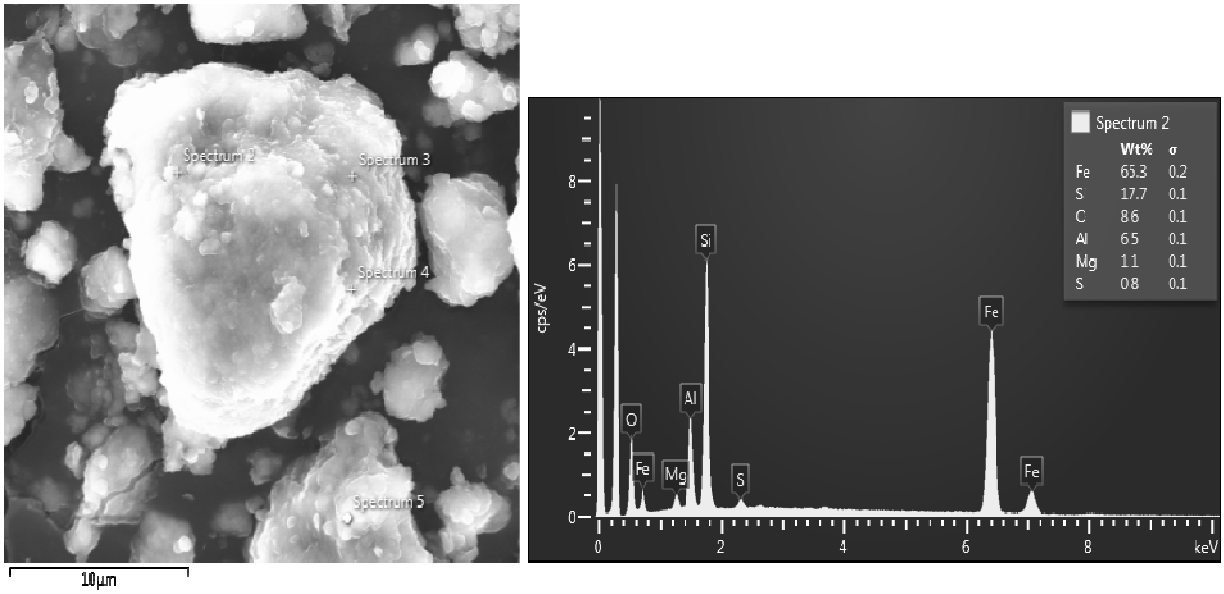

Figure 4 SEM image of composite material BM1 with EDX analysis

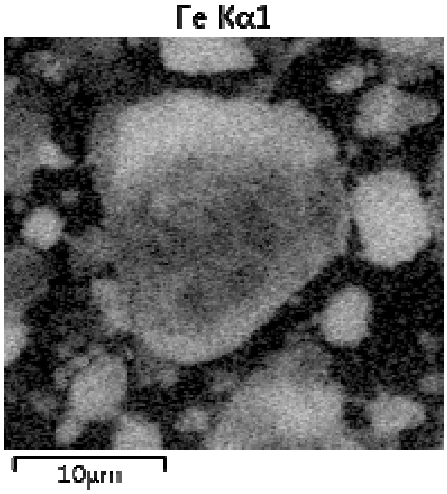

Figure 5 SEM image of composite material BM1 in mapping mode to separate the contrast of iron oxide covering the bentonite surface

The surface properties were also studied by the low temperature nitrogen adsorption method. The hysteresis loop between the adsorption and desorption branches of the investigated samples is an evidence of the presence of mesopores in the structures of the natural bentonite and composites. The hysteresis loop observed for the pure iron oxide was similar to type H1, according to the IUPAC report [35], which is typical for materials with tendency to create agglomerates, what is in agreement with the results obtained from the SEM observations. The present loop is a result of additional sorption process into the interparticles space. The shape of the final parts of the adsorption isotherms of the bentonite and composite materials is related to the occurrence of macropores in studied materials.

Due to the presence of the iron oxide particles, higher volume of adsorbed gas was observed for the BM1 and BM2 materials than for bentonite, Fig. 6, also the value of total pore volume V_a increased after the modification, Table 3. The value of specific surface area S_{BET} of the bentonite increased almost twice after the modification. The value micropore volume V_{micro} is lower for BM1 and BM2, probably due to restrained access of the nitrogen molecules into some of micropores filled by the agglomerated iron oxide nanoparticles. The mesoporous character of the studied sample was also confirmed by the pore size distribution curves, Fig. 7. For the composite materials an increase of the adsorbed volume in the range 2 – 50 nm was observed, what is an evidence of the agglomerated particles precipitated on the surface of bentonite. The distribution curve for BM2 sample is shifted left, to lower values of pore diameters. The presence of smaller pores could point at the presence of smaller iron oxide particles in the samples, what corresponds with the results presented from the Mössbauer spectroscopy

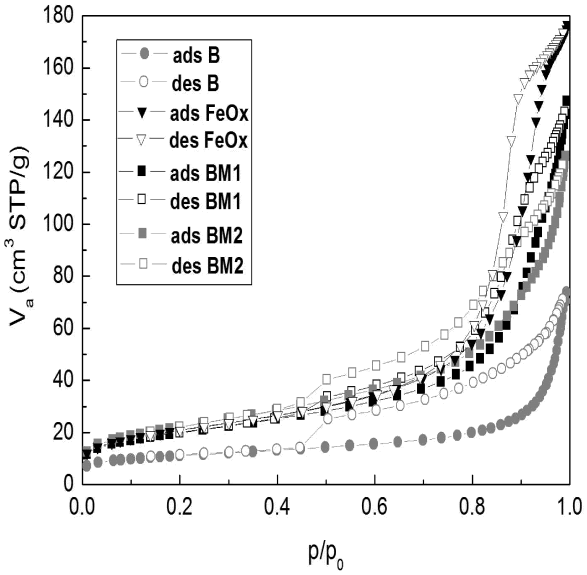

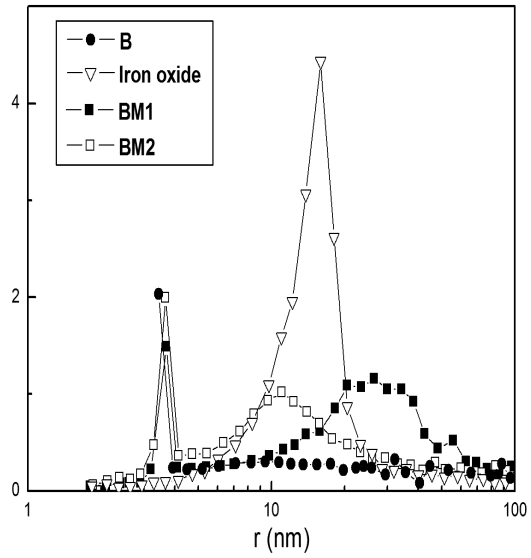

Figure 6 (left) Low temperature nitrogen adsorption and desorption isotherms of composite samples in comparison with natural bentonite and synthetized iron oxide

Figure 7 (right) Pore size distribution curves of composite samples in comparison with natural bentonite and synthetized iron oxide

Table 3 Structural parameters of natural bentonite, iron oxide and composite materials

Sample	S_{BET} (m^2/g)	V_a (cm^3 /g)	V_{micro} (cm^3/g)	S_t (m^2/g)
B	39.4	0.096	0.006	25.4
Iron oxide	75.6	0.266	0.003	67.7
BM1	71.5	0.205	0.003	62.4
BM2	80.8	0.177	0.001	75.1

Pb(II) adsorption

The metal ion uptake increased in the pH range from 3 to 6, the highest metal uptake was observed for pH 7-10, due to the precipitation of $Pb(OH)_2$, Fig. 8. For the next adsorption experiments the optimal pH equal 5 was selected.

The kinetics of the Pb(II) adsorption was studied during the first 40 minutes of experiment. The metal uptake was analysed in eight different time intervals. It followed from the Fig. 9 that the amount of removed Pb(II) was almost stable in the whole studied time interval for both adsorbents. For the equilibrium adsorption, the 24 hour adsorption interval was chosen.

To analyze the kinetics of the adsorption, the pseudo-second-order model was used to interpret the experimental data, Eq (1):

$$\frac{t}{q_t} = \frac{1}{k\,q_e^2} + \frac{1}{q_e}t\,, \qquad (1)$$

where q_e and q_t are the amounts of metal ions adsorbed per unit mass (mg g^{-1}) at equilibrium and at any time t, respectively, k is the rate constant for the adsorption process (g mg^{-1} min^{-1}) [36].

The kinetic parameters for Pb(II) adsorption onto bentonite and composite material BM2 are given in Table 5. These results indicate that the rate limiting step may be a chemical adsorption.

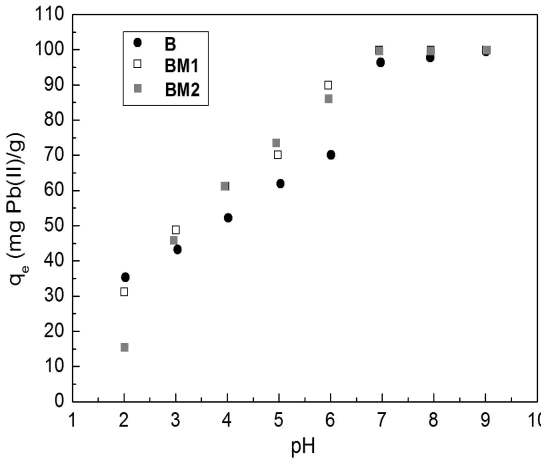

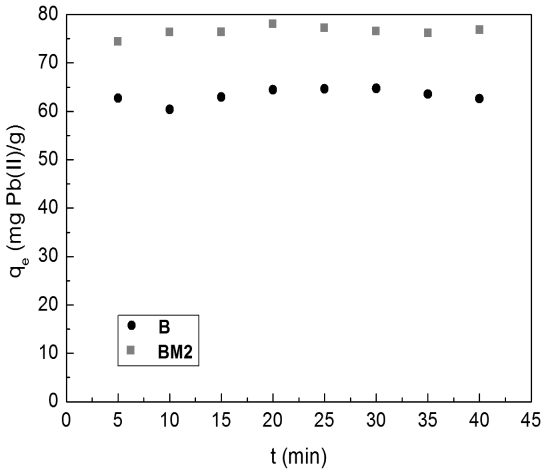

Figure 8 (left) Effect of pH of the solution on the Pb(II) adsorption
Figure 9 (right) Effect of contact time on the Pb(II) adsorption

Table 5 Kinetics parameters of pseudo-second-order model for the adsorption of cadmium (II) onto bentonite and composite material BM2

Sample	k (g/mg .min)	q_e (mg/g)	R^2	$q_{e\ exp.}$ (mg/g)
B	0.205	63.7	0.9989	63.1
BM2	0.563	76.9	0.9998	75.0

$q_{e\ exp.}$ – amount of Pb(II) ions adsorbed per unit mass at equilibrium (obtained from the equilibrium adsorption experiments presented below)

The equilibrium adsorption isotherms are illustrated in Fig. 10. The modified samples adsorbed higher amount of Pb(II) in lower concentration range than bentonite, Figs. 10-11. By increasing the initial Pb(II) concentration in the solution, the saturation of adsorbents was achieved and higher Pb(II) uptake by natural sample was observed.

To analyze the equilibrium data the linearized Langmuir adsorption isotherm was used. The Langmuir model, often applied by various workers for the adsorption of variety of compounds, properly fitted the experimental data in the studied range of the initial concentrations. Its linear form is represented by Eq. (2):

$$\frac{C_e}{q_e}=\frac{1}{Q_0 b}+\frac{C_e}{Q_0}, \qquad (2)$$

where C_e and q_e are equilibrium solute concentration and equilibrium adsorption capacity, respectively, Q_0 is Langmuir constant representing maximum adsorption capacity (amount of adsorbed metal ions per 1 gram of sorbent) and b is adsorption equilibrium constant [37]. The obtained parameters are listed in Table 6.

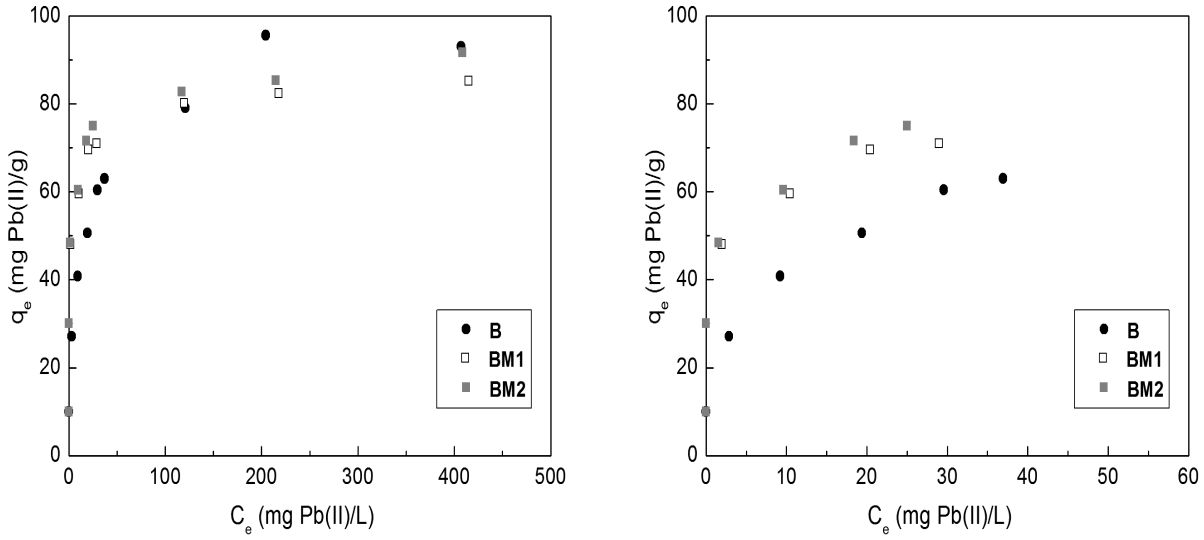

Figure 10 (left) Equilibrium adsorption isotherms for Pb(II) adsorption onto natural bentonite and composite materials
Figure 11 (right) Pb(II) adsorption for lower initial ion concentration range

Table 6 Langmuir parameters for Pb(II) adsorption onto bentonite and composite materials

Sample	Q_0 (mg/g)	b (L/mg)	R^2
B	96.2	0.078	0.9960
BM1	85.5	0.283	0.9995
BM2	90.9	0.228	0.9984

Q_0 – maximum adsorption capacity, b – constant related with the adsorption energy, R^2 – correlation coefficient

Different adsorption rates of natural bentonite and composite materials apparent at low concentrations evoked the further study of their sorption efficiency. The removal of heavy metal cations at low concentrations from aqueous environment is generally difficult. In very low metal concentrations, processes such as precipitation (addition of a base to precipitate hydroxides) are not adequate and sufficient [38]. Due to the complexation with inorganic and organic ligands of the water, the final dissolved concentrations are above those expected according to the thermodynamic solubility products of the precipitates [39]. On the other hand, sorption on the commercially activated carbon is effective, but very expensive [40].

While the equilibrium adsorption capacities q_e of the composite materials were almost equal in the whole investigated concentration range, they were evidently higher in comparison to bentonite, Fig. 11. The effect of Pb(II) adsorption onto bentonite was 63 % , BM1 and BM2 composite material reached 71 and 75 %, respectively.

CONCLUSION

The synthesis of bentonite/iron oxide composites offered to obtain the composite materials, whose properties were affected by the precipitation of maghemite and goethite on the bentonite surface in agglomerated form. The studied composite sorbents showed good affinity to Pb(II) cations, especially for lower initial metal ions concentrations in the solution. They showed to be convenient in disposal of metals cations from the aqueous solutions, where their concentration is very low, but still harmful, as well as for the final purification of pre-treated waste waters. Moreover, magnetic sorbents could be separated from the medium after the adsorption process in high gradient magnetic field [41].

LIST OF SYMBOLS

B_{hf}	hyperfine magnetic field (T)
IS	isomer shift (mm s^{-1})
QS	quadrupole splitting (mm s^{-1})
I	relative spectral area (%)
σ	magnetization (emu g^{-1})
p/p_0	relative pressure (hydrostatic pressure/saturation pressure) (-)
V	adsorbed volume of the nitrogen at the corresponding pressure (cm^3 g^{-1})
S_{BET}	specific surface area (m^2 g^{-1})
V_{micro}	micropore volume (cm^3 g^{-1})
S_t	external surface area (m^2 g^{-1})
V_a	total pore volume (cm^3 g^{-1})
C_0	initial metal ion concentration (mg L^{-1})
m_s	sorbent concentration (g L^{-1})
q_t	amounts of metal ions adsorbed at various times t (mg g^{-1})
t	time (min)
k	rate constant of the pseudo-second-order model for the adsorption process (g mg^{-1} min^{-1})
R^2	coefficient of determination (-)
C_e	equilibrium metal ion concentration (mg L^{-1})
Q_0	Langmuir constant representing maximum adsorption capacity (mg g^{-1})
b	Langmuir sorption equilibrium constant (L mg^{-1})
q_e	amount of metals adsorbed at equilibrium (mg g^{-1})

ACKNOWLEDGEMENT

The authors are thankful for financial support of VEGA grants No. 2/0049/15 and 2/0079/16. Author Z.D. would like to thank to DAAD (Deutscher Akademischer Austauschdienst) for scholarship gained for a short research stay in Germany.

(Received February 2017, accepted March 2017)

REFERENCES

[1] WHO (World Health Organization). Lead poisoning and health. [online] http://www.who.int/mediacentre/factsheets/fs379/en/

[2] Bailey, S.E., Olin, T.J., Bricka, R.M. and Adrian, D.D. (1999). A review of potentially low-cost sorbents for heavy metals. Water Research, vol. 33, pp. 2469-2479.

[3] Bhattacharrya, K.G., Sen Gupta, S. (2008). Adsorption of a few heavy metals on natural and modified kaolinite and montmorillonite: A review. Advances in Colloid and Interface Science, vol. 140, pp. 114-131.

[4] Tahir, S.S., Naseem, R. (2007). Removal of Cr(III) from tannery wastewater by adsorption onto bentonite clay. Separation and Purification Technology, vol. 53, pp. 312-321.

[5] Sanchez, A.G., Ayuso, E.A.,De Blas, O.J. (1999). Sorption of heavy metals from industrial waste water by low-cost mineral silicates. Clay Minerals, vol. 34, pp. 469-477.

[6] Sen Gupta, S., Bhattacharrya, K.G. (2012). Adsorption of heavy metals on kaolinite and montmorillonite: A review. Physical Chemistry Chemical Physics, vol. 14, pp. 6698-6723.

[7] Sousa, F.W., Sousa, M.J., Oliveira, I.R.N., Oliveira, A.G., Cavalcante, R., Fechine, P.B.A., Neto, V.O.S, de Keukeleire, D., Nascimento, R.F. (2009). Evaluation of a low-cost adsorbent for removal of toxic metal ions from wastewater of an electroplating factory. Journal of Environmental Management, vol. 90, pp. 3340-3344.

[8] Binitha, N.N., Sugunan, S. (2006). Preparation, characterization and catalytic aktivity of titania pillared montmorillonite clays. Microporous and Mesoporous Materials, vol. 93, pp. 82-89.

[9] Bouchenafa-Saïb, N., Khouli, K., Mohammedi, O. (2007). Preparation and characterization of pillared montmorillonite: application in adsorption of cadmium. Desalination, vol. 217, pp. 282-290.

[10] Brum, M.C., Capitaneo, J.L., Oliveira, J.F. (2010). Removal of hexavalent chromium from water by adsorption onto surfactant modified montmorillonite. Minerals Engineering, vol. 23, pp. 270–272.

[11] Copcia, V., Hristodor, C., Bilba, N., Popovici, E. (2011). Use of natural and modified clay for Zn^{2+} removal. Revista de Chimie, vol. 62, pp. 195-198.

[12] Galamboš, M., Rosskopfová, O., Kufčáková, J., Rajec, P. (2011). Utilization of Slovak bentonites in deposition of high-level radioactive waste and spent nuclear fuel. Journal of Radioanalytical and Nuclear Chemistry, vol. 288, pp.765-777.

[13] Galamboš, M., Daňo, M., Rosskopfová, O., Šeršeň, F., Kufčáková, J., Adamcová, R., Rajec, P. (2012). "Effect of gamma-irradiation on adsorption properties of Slovak bentonites. Journal of Radioanalytical and Nuclear Chemistry, vol. 292, pp. 481-492.

[14] Lina, J.X., Wang, L. (2011). Treatment of textile wastewater using organically modified bentonite. Desalination and Water Treatment, vol. 25, pp. 25-30.

[15] Wang, W.Q., Feng, Q.M., Dong, F., Li, H., Zhao, X. (2010). Preparation and properties of Fe3O4/clinoptilolite magnetic composite. Wuji Cailiao Xuebao/Journal of Inorganic Materials, vol. 25, pp. 401-405.

[16] Galamboš, M. , Magula, M., Daňo, M., Osacký, M., Rosskopfová, O., Rajec, P. (2012). Comparative study of cesium adsorption on dioctahedral and trioctahedral smectites. Journal of Radioanalytical and Nuclear Chemistry, vol. 293, pp. 829-837.

[17] Galamboš, M., Osacký, M., Rosskopfová, O., Krajňák, A., Rajec, P. (2012). Comparative study of strontium adsorption on dioctahedral and trioctahedral smectites. Journal of Radioanalytical and Nuclear Chemistry, vol. 293, pp. 889-897.

[18] Galamboš, M., Krajňák, A., Rosskopfová, O., Viglašová, E., Adamcová, R., Rajec, P. (2013). Adsorption equilibrium and kinetic studies of strontium on Mg-bentonite, Fe-bentonite and illite/smectite. Journal of Radioanalytical and Nuclear Chemistry, vol. 298, pp. 1031-1040.

[19] Pivarčiová, L., Krajňák, A., Rosskopfová, O., Galamboš, M., Rajec, P. (2015). Adsorption of nickel on andesitic bentonite Lieskovec. Journal of Radioanalytical and Nuclear Chemistry, vol. 304, pp. 851-858.

[20] Krajňák, A., Pivarčiová, L., Rosskopfová, O., Galamboš, M., Rajec, P. (2015). Adsorption of nickel on rhyolitic Slovak bentonites. Journal of Radioanalytical and Nuclear Chemistry, vol. 304, pp. 587-593.

[21] Rosskopfová, O., Pivarčiová, L., Krajňák, A., Galamboš, M., Rajec, P. (2016). Adsorption of nickel on illite/smectite Dolná Ves. Journal of Radioanalytical and Nuclear Chemistry, vol. 307, pp. 179-185.

[22] Chen, Y., Zhu, B., Wu, D., Wang, O., Yang, Y., Ye, W., Guo, J. (2012). Eu(III) adsorption using di(2-thylhexly) phosphoric acid-immobilized magnetic GMZ bentonite. Chemical Engineering Journal, vol.181-182, pp. 387-396.

[23] Hristodor, C.M., Vrinceanu, N., Pode, R., Copcia, V.E., Botezatu, E., Popovici, E. (2013). Preparation and thermal stability of Al_2O_3-clay and Fe_2O_3-clay nanocomposites, with potential application as

remediation of radioactive effluents. Journal of Thermal Analyses and Calorimetry, vol. 111, pp. 1227-1234.

[24] Oliveira, L.C.A., Rios, R.V.R.A., Fabrik, J.D., Sapag, K., Garg, V.K., Lago, R.M. (2003). Clay-iron oxide magnetic composite for the adsorption of contaminants in water. Applied Clay Science, vol. 22, pp. 169-177.

[25] Randelović, M., Purenović, M., Zarubica, A., Purenović, J., Matović, B., Momčilović, M. (2012). Synthesis of composite by application of mixed Fe, Mg (hydr)oxides coatings onto bentonite - A use for the removal of Pb(II) from water. Journal of Hazardous Materials, vol. 199-200, pp. 367-374.

[26] Jesenák, K., Kuchta, Ľ., Guller, L., Fúsková, J. (1997). Physico-chemical Properties of Bentonite "Stará Kremnička - Jelšový potok": I. Particle Size Distribution. Mineralia Slovaca, vol. 29, pp. 439-442.

[27] Jakabský, Š., Lovás, M., Blaško, F. (2004). Utilization of ferromagnetic fluids in minerals processing. The Air Force Academy of General Milan Rastislav Štefánik. Košice. Slovakia. (in Slovak).

[28] Lagarec, K., Rancourt, D.G. (1998). Recoil-Mössbauer spectral analysis software for Windows. Version 02. University of Ottawa, Department of Physics. Canada.

[29] Rouquerol, J., Avnir, D., Fairbridge, C.W., Everett, D.H., Haynes, J.M., Pernicone, N., Ramsay, J.D.F., Sing, K.S.W., Unger, K.K. (1994). Recommendations for the characterization of porous solids (Technical Report). Pure and Applied Chemistry, vol. 66(8), pp. 1739-1758.

[30] Murad E. (1998). The characterization of soils, clays and clay firing products. Hyperfine Interactions, vol. 111, pp. 251-259.

[31] Taylor, G.L., Routsala, A.P., Keeling, Jr. R.O. (1968). Analysis of iron in layer silicates by Mössbauer spectroscopy. Clays and Clay Minerals, vol. 16, pp. 381-391.

[32] Orolínová, Z., Mockovčiaková, A., Dolinská, S., Briančin, J. (2012). Effect of thermal treatment on the bentonite properties. Arhiv za tehničke nauke, vol. 7, pp. 49-56.

[33] Lima, Jr. E., Brandl, A.L., Arelaro, A.D., Goya, G.F. (2006). Spin disorder and magnetic anisotropy in Fe_3O_4 nanoparticles. Journal of Applied Physics, vol. 99, pp. 083908-1-10.

[34] Šucha, V., Galko, I., Madejová, J., Kraus, I. (1996). Mineralogical and crystallochemical characteristics of bentonite from the area of the Zvolenská kotlina Basin (Western Carpathians). Mineralia Slovaca vol. 28, pp. 129–134.

[35] Sing, K.S.W., Everett, D.H., Haul, R.A.W., Moscou, L., Pierotti, R.A., Rouquérol, J., Siemieniewska, T. (1985). Reporting physisorption data for gas/solid systems with special reference to the determination of surface area and porosity. Pure and Applied Chemistry, vol. 57, pp. 603-619.

[36] Erdem, B., Özcan, A., Gök, Ö., Özcan, A.S. (2009). Immobilization of 2,2' dipyridyl onto bentonite and its adsorption behaviour of copper (II) ions. Journal of Hazardous Materials, vol. 163, pp. 418-426.

[37] Ho, Y.S., Chiu, W.T., Wang, Ch.Ch. 2005. Regression analysis for the sorption isotherms of basic dyes on sugarcane dust. Bioresource Technology, vol. 96, pp. 1285-1291.

[38] Balkaya, N., Bektas, N. (2009). Chromium (VI) sorption from dilute aqueous solution using wool. Desalination and Water Treatment, vol. 3, pp. 43-49.

[39] Sanchez, A.G., Ayuso, E.A., De Blas, O.J. (1999). Sorption of heavy metals from industrial waste water by low-cost mineral silicates. Clay Minerals, vol. 34, pp. 469-477.

[40] Hameed, B.H., Din, A.T.M., Ahmad, A.L. (2007). Adsorption of methylene blue onto bamboo-based activated carbon: Kinetics and equilibrium studies. Journal of Hazardous Materials, vol. 141, pp. 819-825.

[41] Štefušová, K., Václavíková, M., Lovás, M., Hredzák, S. (2012). Use of magnetic filtration in waste water treatment. Acta Montanistica Slovaca, vol. 1, pp. 81-84.